born in mind that the averaging applied in the two methods is quite different, ours yielding directly $\langle \sin^2 \alpha \rangle$, whereas the NOE method yields $\langle r^3_{HH} \rangle^{-2}$ which is related to α by complex trigonometric relations. The NOE method weights small HH distances (in this case the planar arrangement) strongly, so that a somewhat smaller angle should be predicted.

Acknowledgment. This work was supported in part by NSF Grants CHE 851128 and CHE 8604007. NMR spectra were recorded at the NMR Facility for Biomedical Studies,[37] supported by NIH Grant RR00292. Our cooperative program in this general area with Professor C. MacLean at the Free University, Amsterdam, has been aided by a NATO travel grant. We are grateful to Drs. Dolf Huis and Gerd van der Zwan of the Free University, Amsterdam, for helpful comments and to Scott Cramer for performing several calculations.

Electrocatalysis at a Novel Electrode Coating of Nonstoichiometric Tungsten(VI,V) Oxide Aggregates

Pawel J. Kulesza[†] and Larry R. Faulkner*[,‡]

Contribution from the Department of Chemistry, University of Warsaw, Pasteura 1, 02-093 Warsaw, Poland, and Department of Chemistry and Materials Research Laboratory, University of Illinois, 1209 West California Street, Urbana, Illinois 61801.
Received September 14, 1987. Revised Manuscript Received March 4, 1988

Abstract: Cycling the potential between 0.8 and −0.4 V vs. SCE in the colloidal mixture of $WO_3 \cdot 2H_2O/WO_3 \cdot H_2O$ existing in 2 M H_2SO_4 at 35 °C causes the electrodeposition of stable, mixed-valent W(VI,V) oxide aggregates on common electrode substrates. Infrared spectroscopy confirmed the presence of H_2O in the deposit and showed that the extent of hydration is lower than in $WO_3 \cdot 2H_2O$. Well-defined redox transitions have been attributed to the reductive formation and oxidative elimination of hydrogen W oxide bronzes in dihydrate portions of the film. Reduction of monohydrate semirigid microstructures in the film is more irreversible and apparently leads to lower substoichiometric W oxides. Depth profiles were determined by Auger electron spectrometry and secondary ion mass spectrometry. The coating is easily permeable to ions, and the dynamics of charge propagation and electrochromism are comparable to those of dihydrate films. The W(VI,V) oxide film catalyzes the electroreduction of bromate to bromide in H_2SO_4. At bare carbon, BrO_3^- is not reduced prior to the onset of hydrogen evolution at about −0.7 V. At the modified surface, a bromate reduction peak appears at about −0.1 V vs SCE. The peak is linear with concentration from 10^{-5} to 10^{-3} M and is nearly diffusion-controlled. Cyclic and rotating disk voltammetry have been employed to characterize the catalytic reaction between BrO_3^- and reduced centers in the film. For typical quantities of the W(VI,V) oxide film ($(1-4) \times 10^{-7}$ mol cm^{-2}), a moderate apparent rate constant of the heterogeneous reaction (2×10^{-4} cm s^{-1}) was found.

Considerable recent effort has been devoted to the preparation and characterization of organic polymers as materials for coating electrode surfaces.[1-3] Potential applications based on the catalysis of electrochemical reactions have provided much of the incentive for this development.[2-8] The attractiveness of such systems is in the combination of advantages from heterogeneous catalysis (particularly those of a catalyst attached to insoluble matrix) together with benefits of a three-dimensional distribution of catalytic centers, normally characteristic of homogeneous catalysis.[8]

One of the important conflicts in these systems concerns the need to distribute electrons rapidly in the microstructure vs the need for the structure to engage in fast redox chemistry with substrate molecules in solution. Almost all catalytic modified electrodes have been developed by immobilizing good redox mediators into the microstructures.[2] Normally, these are simple, coordinatively saturated, and substitutionally inert redox couples, e.g., $Fe(CN)_6^{3-/4-}$, $Mo(CN)_8^{3-/4-}$, and $Ru(NH_3)_3^{3+/2+}$. They are effective as distributors of charge, because they interchange electrons readily among themselves, but they are unpromising in practical terms, because they are not potent catalysts.[8] In one of the most advanced illustrations of electrocatalysis at chemically modified electrodes, Buttry and Anson[5] separated the mediator and catalyst roles in a three-component system, wherein a redox mediator carried electrons rapidly to and from the immobilized, efficient catalyst sites.

Other problems with modified electrodes arise from the lack of chemical stability among the parts of the microstructure.

A reasonable approach is devising novel electrocatalytic surfaces is to consider inorganic matrices,[9-16] through which one could exploit the available information on heterogeneous catalysts and the electronic concepts of solids.[17-20] Inorganic polymeric oxides

* To whom correspondence should be addressed.
[†] University of Warsaw.
[‡] University of Illinois.

(1) (a) Chidsey, C. E. D.; Murray, R. W. *Science* **1986**, *231*, 25. (b) Wrighton, M. S. *Science* **1986**, *231*, 32.
(2) Murray, R. W. *Electroanal. Chem.* **1984**, *13*, 191-369.
(3) Faulkner, L. R. *Chem. Eng. News* **1984**, *52* (9), 28.
(4) Zak, J.; Kuwana, T. *J. Electroanal. Chem.* **1983**, *150*, 645.
(5) Buttry, D. A.; Anson, F. C. *J. Am. Chem. Soc.* **1983**, *105*, 685; **1984**, *106*, 59 and ref 1-6 therein.
(6) Ikeda, T.; Leidner, C. R.; Murray, R. W. *J. Electroanal. Chem.* **1982**, *138*, 343.
(7) Oyama, N.; Anson, F. C. *Anal. Chem.* **1980**, *52*, 1192.
(8) Anson, F. C.; Ohsaka, T.; Saveant, J.-M. *J. Am. Chem. Soc.* **1983**, *105*, 4883.
(9) Humphrey, B. D.; Sinha, S.; Bocarsly, A. B. *J. Phys. Chem.* **1987**, *91*, 586.
(10) Cox, J. A.; Kulesza, P. J. *Anal. Chem.* **1984**, *56*, 1021.
(11) Kulesza, P. J. *J. Electroanal. Chem.* **1987**, *220*, 295.
(12) (a) Ellis, D.; Eckhoff, M.; Neff, V. D. *J. Phys. Chem.* **1981**, *85*, 1225. (b) Itaya, K.; Ataka, T.; Toshima, S. *J. Am. Chem. Soc.* **1982**, *104*, 4767.
(13) (a) Keita, B.; Nadjo, L.; Krier, G.; Muller, J. F. *J. Electroanal. Chem.* **1987**, *223*, 287. (b) Keita, B.; Nadjo, L. *J. Electroanal. Chem.* **1987**, *227*, 265.
(14) Ghosh, P. K.; Bard, A. J. *J. Am. Chem. Soc.* **1983**, *105*, 5691.
(15) Liu, H.-Y.; Anson, F. C. *J. Electroanal. Chem.* **1985**, *184*, 411.
(16) Murray, C. G.; Nowak, R. J.; Rolison, D. R. *J. Electroanal. Chem.* **1984**, *164*, 205.

0002-7863/88/1510-4905$01.50/0

that contain chains of metal centers in different oxidation states are of interest, not only for their significant electrical conductivity but also as materials with defined acid–base properties and oxygen-transfer capabilities that can lead to new patterns of electrocatalytic reactivity. For example, mixed oxides with the perovskite structure have attracted attention as heterogeneous catalysts for different processes, including reduction of nitrous oxide,[21] CO oxidation,[22] or ethylene hydrogenation.[23]

We recently described a general method for the electrochemical preparation of electrodes modified with mixed-valent tungsten(VI,V) oxides.[24] Our work was stimulated by useful characteristics aside from catalysis, particularly the ease of preparation, chemical inertness, stability in strong acids, high porosity, electronic conductivity, and well-defined surface electrochemistry. The films underwent redox processes involving the generation of nonstoichiometric centers, such as hydrogen tungsten oxide bronzes (H_xWO_3, $0 < x < 1$) or lower tungsten oxides (WO_{3-y}, $0 < y < 1$). The extent of hydration and the thickness of the film could be controlled by varying experimental parameters such as temperature and the length of potential cycling during the modification step. Redox transitions appeared to be faster in more hydrated films, but the durability was poorer.

Optimum W oxide microstructures might be heterodispersed or unevenly hydrated, i.e., in having both rigid, less hydrated portions and freer, more aquated ones. In this study, we describe the preparation and behavior of such compromise aggregate phases on conducting substrates.

The promise of these films for electrocatalytic activity rests on the oxygen nonstoichiometry (oxygen vacancies) and on the electronic conductivity.[25-28] Thus, the system can exhibit both high reactivity toward the reduction of a substrate as well as high rates for charge propagation and redox transition. There are parallels between our work and that of Nadjo and co-workers,[13] who have described electrodes modified by polyoxometalates. Our systems differ in physical extent and in chemical character, but there are similarities in the catalytic behavior.

As substrates for catalytic electroreductions at the W(VI,V) oxide modified electrode, oxoanions that require removal of oxide are of interest. We have investigated the reduction of bromate as an example. This reaction is highly irreversible at bare electrodes,[29,30] but it can readily be performed by homogeneous reductants in the presence of catalysts.[30,31] The catalytic effect of W(VI) on the homogeneous reduction of bromate by iodide has been observed.[32] Thermodynamically, BrO_3^- can be reduced in strong acids prior to the redox transitions in W(VI,V) oxides; hence the electrochemically generated hydrogen tungsten bronzes or lower tungsten oxides may catalyze the electrochemical reduction of bromate. Translation of the homogeneous EC catalysis[33] to the heterogeneous case is therefore possible.

In this paper, we will show that very effective catalysis is indeed observed. Carbon substrates were used as the base electrodes because bromate reduction does not occur at the bare substrate, at least not before the onset of hydrogen evolution at about −0.7 V. Hence, the role of the modifying film in the electrocatalysis becomes apparent readily. The results presented here are of interest not only for their relevance of the analytical prospects for monitoring bromate but also because they concern the general promise of the nonstoichiometric mixed oxide films for catalyzing the electroreductions of oxo-substrates, such as inorganic anions or certain organic molecules.

Experimental Section

The electrochemical experiments were performed with an IBM Instruments EC-225 or a Bioanalytical Systems BAS-100 potentiostat. Rotating disk voltammetry was done with an ASR Rotator (Pine Instrument Co.) fitted with a glassy carbon disk having a geometric area of 0.50 cm^2. All experiments were carried out in a three-electrode configuration. Potentials were measured and reported vs the saturated calomel electrode (SCE).

All chemicals were commercial materials of the highest available purity (ACS Reagent Grade or Puratronic) and were used as received. The house distilled water was further treated with a Milli-Q water purification system.

Solutions were deaerated for at least 5 min prior to the electrochemical experiments with use of prepurified N_2 saturated with water. A nitrogen atmosphere was maintained over the solution at all times. Unless otherwise stated, experiments were conducted at room temperature, 22 ± 2 °C.

A Kel-F sealed glassy carbon substrate from Bioanalytical Systems, with a geometric area of 0.071 cm^2, was used for most voltammetric experiments. Prior to modification, such electrodes were cleaned and polished as described elsewhere.[24] The electrode modification did not require very careful pretreatment of the glassy carbon.[24]

Unless otherwise stated, the modification of a clean substrate was accomplished by a 4-h cycling of the potential at 50 mV s^{-1} between −0.4 and 0.8 V in the pale yellow colloidal mixture of $WO_3 \cdot 2H_2O$ and $WO_3 \cdot H_2O$. The mixture was freshly prepared by dissolution of 5 mL of 0.2 M $Na_2WO_4 \cdot 2H_2O$ in 45 mL of 2.2 M H_2SO_4 at 35 ± 2 °C.

Film thicknesses were measured with an Alpha-step profilometer (Tencor Corp.) as described earlier.[24]

In order to prepare samples for Auger electron spectrometry (AES) or secondary ion mass spectrometry (SIMS), the electrodeposition was performed on pyrolytic graphite disks from Union Carbide (Chicago, IL) as detailed elsewhere.[24]

Auger electron spectra were recorded on a Physical Electronics Model 595 Auger electron spectrometer and secondary ion mass spectrometry data were obtained on a Cameca Instruments IMS 3F ion microanalyzer. These measurements were made with previously reported beam characteristics.[24]

Visible absorption spectra were recorded for films deposited on SnO_2-coated glass slides (PPG Industries, "Nesa", 10–20 Ω/square). A Hewlett-Packard Model 8450A diode array spectrophotometer was used in the manner previously reported.[24]

Infrared spectra were taken with a Zeiss Model UR-20 spectrophotometer. For these measurements, the tungsten oxide was scraped from the graphite electrodes as reported by Reichman and Bard.[34] To make pellets with KBr, a milligram of a finely ground sample was intimately mixed with about 100 mg of dried KBr powder. Special attention was paid to prepare homogeneous samples of similar weight. For quantitative measurements, known and controlled quantities of KBr and the test sample were taken. Additional IR measurements of $Na_2WO_4 \cdot 2H_2O$, and of this salt with graphite powder, suggested that there was no interference from the graphite residues in the region of 1300 to 4000 cm^{-1} that was of our concern.

Results and Discussion

Designing a successful heterogeneous electrocatalyst required careful consideration of the physical and chemical properties of W oxides. Since only in strong acids do W(VI,V) oxide coatings remain stable and provide high rates of charge propagation,[25-28,34] our experiments were generally done in 2 M H_2SO_4. The next important factor was the degree of hydration and the porosity of

(17) Cousidine, D. M. Ed. *Van Nostrands Scientific Encyclopedia*; Van Nostrand Reinhold: New York, 1976; p 447.
(18) Tamura, H.; Yoneyama, H.; Matsumoto, Y. *Electrodes of Conductive Metallic Oxides*; Trasatti, S., Ed.; Elsevier: Amsterdam, 1980; Chapter 6.
(19) Kazanski, V. B. *Kinet. Katal.* **1977**, *18*, 43.
(20) Calvo, E. J.; Drennan, J.; Kilner, J. A.; Albery, W. J.; Steele, B. C. H. *Proceedings of the Symposium on the Chemistry and Physics of Electrocatalysis*; McIntyre, J. D. E., Weaver, M. J., Yeager, E. B., Eds.; The Electrochemical Society: Pennington, NJ, 1984; Vol. 84-12, pp 489-511.
(21) Voorhoeve, R. J. H.; Remeika, J. P.; Johnson, D. W., Jr. *Science* **1972**, *177*, 353; **1973**, *180*, 62.
(22) Tascon, J. M. D.; Tejuca, L. G. *J. Chem. Soc., Faraday Trans. I* **1981**, *77*, 591.
(23) Petunchi, J. O.; Nicastro, J. L.; Lombardo, E. A. *J. Catal.* **1981**, *70*, 356.
(24) Kulesza, P. J.; Faulkner, L. R. *J. Electroanal. Chem.*, in press.
(25) Cotton, F. A.; Wilkinson, G. *Advanced Inorganic Chemistry, A Comprehensive Text*; Wiley: New York, 1980; p 850.
(26) Weisman, P. J.; Dickens, P. G. *J. Solid State Chem.* **1973**, *6*, 374.
(27) Crandall, R. S.; Faughnan, B. W. *Appl. Phys. Lett.* **1976**, *28*, 95.
(28) Faughnan, B. W.; Crandall, R. S. *Appl. Phys. Lett.* **1975**, *27* 275.
(29) Rozhdestvenskaya, Z. B.; Songina, O. A. *J. Anal. Chem. USSR* **1960**, *15*, 155.
(30) Toporova, V. F.; Vekslina, V. A. *J. Anal. Chem. USSR* **1975**, *30*, 271.
(31) Toporova, V. F.; Vekslina, V. A.; Chovnyk, N. G. *J. Anal. Chem. USSR* **1973**, *28*, 856.
(32) Wolff, C. M.; Schwing, J. P. *Bull. Soc. Chim. Fr.* **1976**, 679, 675.
(33) Bard, A. J.; Faulkner, L. R. *Electrochemical Methods*; Wiley: New York, 1980.
(34) Reichman, B.; Bard, A. J. *J. Electrochem. Soc.* **1979**, *126*, 583, 2133.

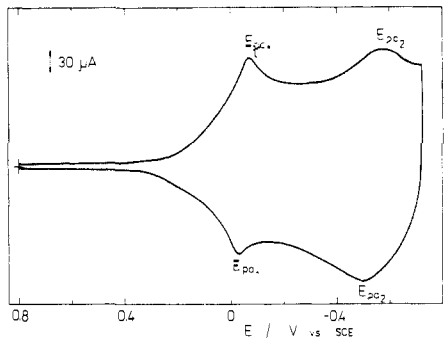

Figure 1. Steady-state cyclic voltammogram of the W(VI,V) oxide deposit on glassy carbon in 2 M H_2SO_4. Modification was performed from the sodium tungstate dihydrate solution as described in the Experimental Section. Scan rate, 50 mV s^{-1}; geometric area of the electrode, 7.1 mm^2.

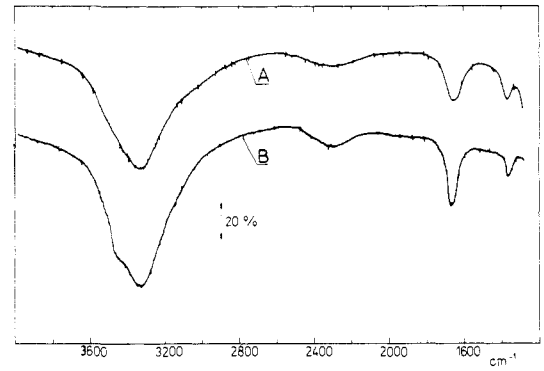

Figure 2. IR spectra of (A) the W(VI,V) oxide coatings prepared as described in the Experimental Section and scraped from the electrode substrate, (B) of $WO_3 \cdot 2H_2O$.

the film. With a gradual increase of temperature from 15 to 90 °C the film converted, in practice irreversibly, from dihyrate to monohydrate.[24,34,35] In the latter form, redox transitions appeared to be slower, but the stability was better.[24,34] Thus, our optimum modification procedure involved electrodeposition coupled with sol-gel aggregation upon reduction.[24] We worked from the pale-yellow colloidal mixture of $WO_3 \cdot 2H_2O$, with some $WO_3 \cdot H_2O$, existing in 2 M H_2SO_4 at 35 °C.[36] The films were grown slowly by potential cycling as described in the Experimental Section. This approach is known to favor formation of porous, hydrated metal oxide coatings.[37] When thickness measurements were made by profilometer, a mean value of 2400 ± 300 Å was obtained.

Physicochemical Identity and Voltammetric Behavior of the Films. Figure 1 shows the cyclic voltammogram obtained in 2 M H_2SO_4 with a glassy carbon electrode coated with the oxide deposit. The film underwent a well-defined and well-separated double reduction in the range from +0.8 to −0.7 V, and the reduced film showed a corresponding double oxidation. The reduction peaks are observed at E_{pc1} = −0.090 V and E_{pc2} = −0.580 V, whereas the oxidation peaks appear at E_{pa1} = −0.045 and E_{pa2} = −0.500 V.

Comparison of these results with those previously reported by us,[24] dealing with the electrochemical behavior of dihydrate, monohydrate, and anhydrous W(VI,V) oxide coatings, suggests that the pattern in Figure 1 is characteristic for a coating somewhat less hydrated than the dihydrate. With films of lower water content, the E_{pc1} and E_{pc2} reduction peaks are shifted toward more negative values.[34,35] Further, IR measurements of pellets prepared with the W(VI,V) oxides (in air, practically WO_3) scraped from the electrode show that the amount of water in the films is lower than that in the dihydrate standard,[36] $WO_3 \cdot 2H_2O$. A typical infrared spectrum of the WO_3 films (Figure 2, curve A) clearly indicates the presence of water via its characteristic peaks near 1650 and 3500 cm^{-1}.[34,38] The heights of these peaks in various samples should express differences in water content. Indeed, when the W(VI,V) oxide film was prepared by electrodeposition at lower temperature, i.e., at 17 °C, the heights increased virtually to levels characteristic for authentic dihydrate $WO_3 \cdot 2H_2O$ (Figure 2, curve B), which was prepared according to Freedman,[36] except for being precipitated from 2 M H_2SO_4 instead of 3 M HCl.

The extent of hyration of the W(VI,V) oxide coatings prepared at 35 °C should be related to the water content in the pale-yellow stable phase of WO_3 that exists as colloidal suspension in H_2SO_4 (i.e., in the mixture for modification). In order to test this hypothesis, an additional voltammetric experiment was performed with a glassy carbon electrode that had been modified by mechanical dispersion, i.e., by polishing the electrode surface with the WO_3 filtrate (from the colloidal precipitate obtained at 35 °C in 2 M H_2SO_4), in the manner proposed by Kuwana et al. for various metal oxides.[24,39] Indeed, such glassy carbon modified electrodes exhibited voltammetric behavior virtually identical (particularly in terms of E_{pc1}, E_{pa1}, E_{pc2}, and E_{pa2}) with the one shown in Figure 1. This behavior contrasts significantly with that of both the authentic monohydrate, which does not show these peaks, and the authentic dihydrate, which has a markedly narrower separation between the two sets of peaks.[24]

An estimation of the water content in the pale-yellow WO_3 phase was attempted via IR spectroscopy. In order to avoid dissolution or changes in the extent of hydration of WO_3, these filtrates were rinsed with diluted 0.1 M H_2SO_4, rather than with distilled water. To perform comparative IR measurements and to estimate the water content in the pale-yellow WO_3 phase, two colloidal suspensions, both the white dihydrate and the pale-yellow, were prepared at 16 and 35 °C, respectively, and subsequently filtered, rinsed, and dried. The peak at ca. 1650 cm^{-1} was used for the evaluation, and it was assumed that Beer's law was obeyed. A base-line method for determination of absorbance, in which the contribution from aquated H_2SO_4 was assumed to be constant, was employed. The extent of hydration was found to be roughly 1.8, which may indicate structural heterogeneity of the phase.

When $WO_3 \cdot H_2O$ is brought into contact with 2 M H_2SO_4, the solid does not disperse readily to form a colloid system, and therefore is lyophobic.[40] In contrast, the lyophilic $WO_3 \cdot 2H_2O$ produces a colloidal dispersion spontaneously. At present, there is not enough evidence to assume the formation of micelle-like polydispersions in the pale-yellow WO_3 phase, but the existence of two portions, the rigid lyophobic monohydrate and the redox-facile dihydrate, can be expected.

The formation of the pale-yellow, incompletely hydrated WO_3 colloid takes place not only at 35 °C but also as a result of aging, e.g., for 48 h in 2 M H_2SO_4, of the white dihydrate suspension, even at 16 °C. The effect was confirmed both visually and with the use of IR spectroscopy. When the time of the aging was increased to 96 h, no further changes in the level of hydration were observed, implying that a metastable phase was formed. As before for filtrates, we estimated a number of water molecules associated with WO_3, z, and found that in all cases z = 1.8 ± 0.1. In contrast, the aging of the dihydrate aggregates formed as W(VI,V) oxide coatings on carbon electrodes was much less pronounced. There were no changes in the positions of voltammetric peaks during 48 h of repetitive cycling of the electrode potential from 1.0 to −0.5 V in 2 M H_2SO_4 at 22 °C. This improved stability of surface films is not surprising, since the solution phases are metastable sols, whereas the deposited films are probably semirigid inorganic gel aggregates,[24] typically consisting of water trapped within a

(35) DiPaola, A.; DiQuarto, F.; Sunseri, C. *Corrosion Sci.* **1980**, *20*, 1069, 1079.
(36) Freedman, M. L. *J. Am. Chem. Soc.* **1959**, *81*, 3834.
(37) (a) Burke, L. D.; O'Sullivan, E. J. M. *J. Electroanal. Chem.* **1981**, *117*, 155. (b) Burke, L. D.; Twomey, T. A. M.; Whelan, D. P. *J. Electroanal. Chem.* **1980**, *107*, 201.
(38) Hurditch, R. J. *Electron Lett.* **1975**, *11* (7), 142.
(39) Dong, S.; Kuwana, T. *J. Electrochem. Soc.* **1984**, *131*, 813.
(40) (a) Levine, I. N. *Physical Chemistry*; McGraw-Hill: New York, 1978; pp 341–345. (b) Atkins, P. W. *Physical Chemistry*, 2nd ed.; W. H. Freeman: New York, 1982; pp 842–847.

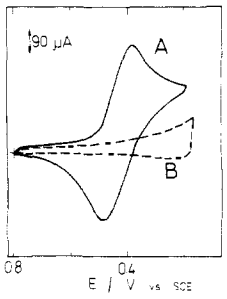

Figure 3. Cyclic voltammograms recorded in 2 M H_2SO_4 with a glassy carbon electrode coated with the W(VI,V) oxide deposit of Figure 1 in the presence (A) and absence (B) of 2 mM $K_3Fe(CN)_6$. Scan rate, 100 mV s^{-1}; geometric area of the electrode, 7.1 mm^2.

three-dimensional network of tiny crystals held together by van der Waals forces.[40]

We[24] have interpreted voltammetry like that in Figure 1 in terms of two distinct, parallel electrode processes: (a) hydrogen uptake to give the hydrogen tungsten oxide bronzes,[41-43] which may be written as $WO_3 + xH^+ + xe^- \rightleftarrows H_xWO_3$ ($0 < x < 1$), and (b) the reduction of W(VI) to lower tungsten oxides,[44] which can be described as $WO_3 + 2ye^- + 2yH^+ \rightleftarrows WO_{3-y} + yH_2O$ ($0 < y < 1$). In the case of dihydrate coatings, the insertion of a proton upon a valence adjustment of W (i.e. bronze formation) and proton transport via H_3O^+ exchange between adjacent water molecules are relatively unhindered.[34,41-44] For monohydrate or anhydrous W oxides, the mobility of H^+ is significantly lowered, and the breaking of tungsten–oxygen bonds to form oxygen ion vacancies, and thus substoichiometric W oxides, could start to predominate.[41,44] For our unevenly hydrated coatings (prepared by electrodeposition at 35 °C), both types of redox process are to be expected. The appearance of two sets of well-developed and well-separated peaks, E_{pc1}/E_{pa1} and E_{pc2}/E_{pa2}, on an underlying broad background supports this hypothesis. Since the reduction to hydrogen tungsten bronzes takes place at generally more positive potentials than the formation of substoichiometric lower W oxides,[41-43] one can understand the peaks at E_{pc1} and E_{pc2} in terms of the reductive absorption of hydrogen into the oxide. The literature indicates the existence of two stable phases of the hydrogen W bronzes, $H_{0.18}WO_3$ and $H_{0.35}WO_3$.[45] Thus, the E_{pc1} peak should be, as before in the case of dihydrate coatings,[24] attributed to formation of $H_{0.18}WO_3$. The E_{pc2} current at potentials about 500 mV more negative than E_{pc1}, cannot be wholly attributed to the formation of $H_{0.35}WO_3$. Judging from the appearance of significant background currents at potentials more negative than −0.2 V and referring to our previous report,[24] we believe that reduction to the substoichiometric ("blue") W oxides (WO_{3-y}) also contributes substantially to the overall process.

Integration of the voltammetric peak at E_{pc1}, above an estimated base line, yielded a charge of 4.1 mC cm^{-2}, which approximately corresponds to 2.4×10^{-7} mol cm^{-2} of catalytic WO_3/H_xWO_3 centers, or about 2400 catalyst monolayers. In this calculation, it is assumed that for charge balance to be maintained, the creation of 1 mol of $H_{0.18}WO_3$ phase requires injection of 0.18 mol of electrons.

Permeability, Stability, and Reversibility of Redox Transitions. Efficient electrocatalysis requires ready access of the reactant to catalytic sites within the film. Physical permeability was probed via the voltammetric behavior of the $Fe(CN)_6^{3-/4-}$ couple. The cyclic voltammogram (Figure 3) recorded in 2 M H_2SO_4 at 200 mV s^{-1} reveals a measured $E^{\circ\prime}$ = 0.435 V, which is the value observed in the same solution at platinum. The peak current scales with the square root of scan rate in the range from 10 to 300 mV s^{-1}, and the waveforms are characteristic for a diffusion-limited process. The differences between the peak potentials were 64, 72, and 86 mV at 50, 100, and 200 mV s^{-1}. Further, the peak current ratios remained equal to unity. Thus, the electrode reaction is almost electrochemically reversible. At potentials more positive than 0.3 V, the film behaves like a semiconductor,[24,44] and it is unlikely that there would be such reversibility if the electrode process were confined to the oxide/solution interface. Thus we conclude that the film is readily permeable to ferri/ferrocyanide.

Table I. Voltammetric Parameters for Reduction Peaks at E_{pc1}[a]

v/mV s^{-1}	$i_{pc1}/\mu A$	E_{pc1}/V	$i_{pc1}v^{-1}/\mu A$ mV s^{-1}
500	1120	−0.110	2.24
200	496	−0.100	2.48
100	257	−0.095	2.57
50	131	−0.090	2.62
20	53.1	−0.087	2.66
10	26.9	−0.085	2.69
5	13.6	−0.085	2.72

[a] Experimental conditions as for Figure 1, except that the scan rate, v, is varied.

The characteristics of the cyclic voltammogram in Figure 3 do not change qualitatively even when the film is ca. 6 times thicker, i.e., with a charge at E_{pc1} of 24 mC cm^{-2}. However, the thicker film causes a 20% decrease in the voltammetric peak currents and an increase in the peak separation from 64 to 105 mV at 50 mV s^{-1}. The virtually unchanged $E^{\circ\prime}$ value at the modified electrode vs bare carbon suggests that there is no specific interaction between the coating and ferro- or ferricyanide.

The stability of the coating was tested by measuring a decrease of the voltammetric peak current at E_{pc1} during various experiments in 2 M H_2SO_4. Each measurement was performed at least three times with a freshly prepared W(VI,V) oxide film on a selected glassy carbon substrate. Solutions were stirred by bubbling nitrogen through them. After simply soaking the electrode in the electrolyte for 4 h, a decrease of 22 ± 4% was observed in the current. In the case of potential cycling from −0.45 to 0.8 V at 50 mV s^{-1} for 4 h, a decrease of 12 ± 3% took place. No changes in the positions of peaks were observed. The error bars given above represent one standard deviation about the mean.

The increased stability of the W(VI,V) oxide coatings described here, when compared to dihydrate films,[24] apparently results from the structural heterogeneity of the assemblies. The presence of the already postulated, less hydrated, lyophobic portions in the W oxide aggregates seems to decrease solubility and increase the overall durability of the coating.

At scan rates up to 500 mV s^{-1}, the voltammetric currents measured in the potential range from 0.8 to −0.7 V are proportional to scan rate, as expected for surface processes. The effect of v on the peak current at E_{pc1} is summarized in Table I for a glassy carbon modified electrode in 2 M H_2SO_4. In the range from 5 to 500 mV s^{-1}, the function $i_{pc1}v^{-1}$ is nearly independent of v, changing by only about 18%. The decrease at faster scan rates may reflect limitations associated with charge propagation in the film. For v = 5–100 mV s^{-1}, the peak potentials E_{pc1} and E_{pa1} remain constant, and the difference between them is 40–45 mV. At higher v, a wider splitting is observed. At all potentials where redox transitions are observed (<0.3 V), tungsten exists in multiple oxidation states, and this feature is known to be responsible for the electronic conductivity of the mixed valent metal complexes.[46,47] For tungsten bronzes, conductivity increases with the degree of reduction.[25,48]

The E_{pc1} and E_{pa1} peaks are not perfectly symmetrical, probably because of the background currents and kinetic limitations in the redox transitions. The peaks are quite broad. It is not clear to what extent the broadening is due to repulsive interactions between the electroactive sites or to the electrochemical nonequivalence

(41) Dickens, P. G.; Hurditch, R. J. *Nature (London)* **1967**, *215*, 1266.
(42) Benson, J. E.; Kohn, H. W.; Boudart, M. *J. Catal.* **1966**, *5*, 307.
(43) Glemser, O.; Neumann, K. *Z. Anorg. Chem.* **1951**, *265*, 288.
(44) Hobbs, B. S.; Tseung, A. C. C. *J. Electrochem. Soc.* **1975**, *122*, 1174.
(45) Dickens, P. G.; Moore, J. H.; Neild, D. J. *J. Solid State Chem.* **1973**, *7*, 241.
(46) Buravov, L. N.; Stepanova, R. N.; Khidekel', M. L.; Shchegolev, I. F. *Dokl. Akad. Nauk SSSR* **1972**, *4*, 819.
(47) Little, W. A. *Phys. Rev.* **1964**, *134A*, 1416.
(48) Hagenmuller, P. *Comprehensive Inorganic Chemistry*, Trotman-Dickenson, A. F., Executive Ed.; Pergamon Press: Oxford, 1973; Vol. 4, Chapter 50, pp 541–563.

of the sites. The redox behavior does not fit the Nernstian relationship,[49] as is evident by the different values for E_{pc1} and E_{pa1} and the somewhat differing slopes obtained for the cathodic and anodic peaks vs scan rate.

The oxidation peak at E_{pa1} is broader than the reduction peak at E_{pc1}, but the peak current still scales linearly with the sweep rate up to 500 mV s^{-1}. The area under the E_{pa1} peak is 0.92 of the area of that at E_{pc1}. The areas for the cathodic and the anodic peaks should be equal, as they represent formation and oxidation of the hydrogen W bronze phase. The difference apparently results from the difficulty in determining the base line. The difference in breadth of the oxidation and reduction peaks is an effect also observed for polymer films containing redox centers on electrodes. It can arise from interactions between sites or from inequivalences of sites.[5]

During the overall cathodic reduction, the film changes color, from a transparent yellow in the neutral state to blue in the reduced state. The approximate thickness of the film, determined from profilometry, was about 2000 Å. The absorption spectrum of a reduced film on SnO_2-coated glass has peaks with λ_{max} at 610 and 355 nm. Oxidation of the reduced film changes the spectrum; the peak at 610 nm largely disappears, while that at 355 nm basically remains unchanged. The positions of these peaks are analogous to those previously reported by us[11,24] for the dihydrate coatings, except that in the latter case the redder absorption peak, characteristic for the reduced film, tends to appear 20–30 nm earlier, at about 585 nm.

The kinetics of coloration and bleaching directly reflect the dynamics of redox transitions in the films. About 2–3 s were required for visually distinct coloring of the film at −0.4 V and for bleaching it by oxidation at 0.8 V. In cyclic voltammetric experiments with the modified SnO_2-coated glass, color changes were visible at 50 mV s^{-1}. Electrochromism appeared to be reversible during at least 40 cycles of potential steps between 0.8 and −0.4 V.

Mechanism of Charge Propagation. Good understanding of the dynamics and nature of charge propagation in the films is of particular importance to efficient electrocatalysis. Reichman and Bard[33] assumed that the discharge of hydrogen ions and the concurrent diffusion of hydrogen atoms within the oxide were rate-determining for the reduction of WO_3 films prepared either by vacuum evaporation or by anodic oxidation of W. In their approach, the mass transfer of protons in solution and the transport of electrons through the films were considered to be relatively fast. The strong resemblance between the electrochemical behavior of our mixed-valent W(VI,V) oxide coatings[24] and the anodic WO_3 films[34] allows an extension of this view to our system. The dihydrate portions of the W(VI,V) oxide film are apparently as fully hydrated as anodic WO_3. Thus the whole process in the film is governed by Fick's laws,[34] and a value of the effective diffusion coefficient, $D_{H\text{-}eff}$, can be easily derived from chronocoulometric charge Q vs time curves in the manner described by Reichman and Bard[34] and by Chambers.[50]

In the chronocoulometric experiment, a glassy carbon electrode modified with a W(VI,V) oxide film of 230-nm dry thickness was transferred to 2 M H_2SO_4 and equilibrated at 0.8 V; then a 100-ms potential pulse to −0.25 V was applied, and the charge–time curve was recorded. The step potential was approximately 150 mV more negative than E_{pc1}; this assured a reasonably quick establishment of diffusion-limited behavior. After a forward step time t_f, the electrode potential was returned to its initial value for another period of duration t_f before the experiment was terminated.[51] Both the forward and reverse parts of the Q–t curve and the Anson plot (Figure 4) could be reproduced in at least 10 consecutive experiments.

Diffusion coefficients were evaluated by two means. The approach proposed by Chambers[50] is based on the time $t_{0.5}$ when

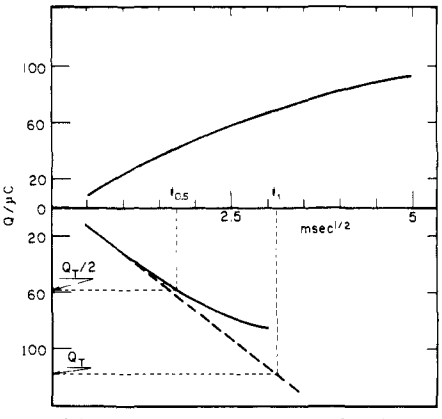

Figure 4. Typical forward and reverse Anson plots for the chronocoulometry at the W(VI,V) oxide electrode in 2 M H_2SO_4. Evaluation of $t_{0.5}$ and t_i is shown via the dotted lines.

Table II. Dependence of $D_{H\text{-}eff}$ on the Film Thickness[a]

d/nm[b]	τ/ms	$10^8 D_{H\text{-}eff}$/cm^2 s^{-1}
160	20	5.0
230	60	3.5
310	130	3.0
420	350	2.0

[a] In 2 M H_2SO_4. [b] Estimated from profilometry measurements on modified Atomergic glassy carbon slides.

$Q = Q_T/2$, where Q_T is the total charge consumed in exhaustive electrolysis. For a film of uniform thickness d, one can define a characteristic diffusion time $\tau \equiv (2d)^2/D_{H\text{-}eff}$, which can be shown[50] to be $(8^2/\pi)t_{0.5}$. Alternatively, τ can be evaluated as $(16/\pi)t_i$, where t_i is the time where the extrapolated Cottrell line (Q vs $t^{1/2}$) intersects the $Q = Q_T$ axis (Figure 4). The results agreed within 10 ms, and an average τ-value of 60 ms was obtained. The resulting value of $D_{H\text{-}eff} = 4 \times 10^{-8}$ cm s^{-1} was consistent with previous reports for anodic WO_3 films.[34]

Due to difficulties in determing the actual number of electrons transferred and the concentration of electron exchange sites, no attempt was made to evaluate $D_{H\text{-}eff}$ from the Cottrell slopes of chronocoulometric Anson plots. In view of previous findings[34] about the electrochromism in sub-dihydrate tungsten oxides, showing that bleaching (oxidation) of the reduced centers is slower than their formation, the reverse step (oxidation) was used in the analysis. Indeed, effective electrocatalysis would require both steps to be kinetically fast.

In a different series of chronocoulometric measurements, diffusion coefficients were determined for a few film thicknesses of the oxide coating on glassy carbon (Table II). The experimental details were as given above. Consistent τ values were always derived from the chronocoulometric data with use of the two analysis methods described above. The diffusion coefficients generally decreased with increasing thickness of the coating. This behavior may be attributed to some structural changes or a lower permeability to hydrogen-transport in thicker films.

Surface Analysis/Depth Profiles. Surface measurements were performed in order to determine the elemental composition and purity of films prepared under standard conditions. The presence of W, O, and S was established by AES. The latter element originated from the H_2SO_4 electrolyte and was apparently incorporated into the film during electrodeposition. As previously reported by us for dihydrate coatings,[24] AES did not show Na as a major component (even though the mixture for modification contained $Na_2WO_4 \cdot 2H_2O$), implying that the film was not a sodium tungsten bronze. SIMS was used to analyze for minor components. A typical spectrum of the film showed (besides W, O, and S) Na, K, and sometimes traces of Mo as impurities. Since the relative ion yields of elements vary extensively, a quantitative estimate of impurities was not attempted.

Changes in the composition of the film could be seen from AES depth profiles (Figure 5). Three characteristic regions exist: (1) the outermost surface region, ca. 20–40 nm, enriched with S (from

(49) Laviron, E. *Bull. Soc. Chem. Fr.* **1967**, 3717; *J. Electroanal. Chem.* **1972**, *39*, 1.
(50) Chambers, J. Q. *J. Electroanal. Chem.* **1981**, *130*, 381.
(51) Anson, F. C. *Anal. Chem.* **1966**, *38*, 54.

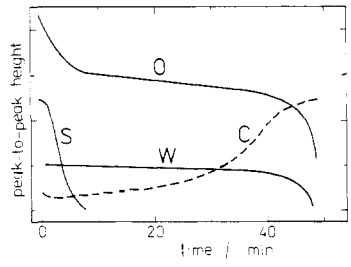

Figure 5. Auger depth profiles for the standard W(VI,V) oxide film on pyrolytic graphite. Original film thickness, ca. 2500 Å.

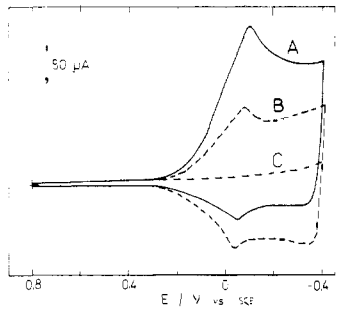

Figure 6. Cyclic voltammograms for the reduction of bromate at (A) glassy carbon/W(VI,V) oxide and (C) bare glassy carbon electrodes; the dashed line (B) is the cyclic voltammogram for bromate-free solution at the W(VI,V) oxide electrode. Bromate concentration, 2 mM; electrolyte, 2 M H_2SO_4; scan rate, 50 mV s^{-1}; substrate area, 7.1 mm^2. The reverse scan on curve C was deleted for simplicity.

H_2SO_4); (2) the bulk of the film, which has an even distribution of the elements; and (3) a transition region in which carbon from the substrate becomes increasingly visible. The outermost region (1) exhibits an almost flat distribution of W, but not of O. The relative signal for O at the surface is larger and gradually decreases with increasing depth. This observation is consistent with the idea that the outermost layers contain SO_4^{2-}.

Electrocatalytic Reduction of Bromate. When one considers the voltage gain that might be realized in catalysis, the E_{pc1} peak that appears in voltammetry at less negative potentials is of special interest. This peak signals the advent of both metallic conductivity and a new type of reducing center, so one could expect the most effective electrocatalysis to begin at roughly E_{pc1}. Since E_{pc1} and E_{pc2} are separated by about 500 mV, any overlap of corresponding catalytic effects is minimized.

The survival of the electrochemically deposited W oxide films for long periods allowed us to examine their behavior as three-dimensional catalytic arrays. The bromate reduction is totally irreversible at bare glassy carbon and does not take place prior to the discharge of hydrogen (Figure 6C). The behavior at the W(VI,V) oxide modified electrode is quite different. A distinct peak appears for BrO_3^-, and its position (Figure 6A) relative to E_{pc1} (Figure 6B) indicates that the electrochemically generated hydrogen W bronzes in the coating reduce BrO_3^-. The fact that the bromate attenuates the oxidation peak at E_{pa1} supports this idea.

The effects of scan rate on the catalyzed bromate reduction peak are summarized in Table III. In the range from 5 to 500 mV s^{-1}, the current function $i_{pc}v^{-1/2}$ is nearly independent of v, changing by only about 10%, which indicates that the current is limited mostly by the diffusion of bromate to the electrode surface. At 1000 mV s^{-1}, the current function decreases by another 15–17%, which suggests the onset of a limitation on the catalytic rate. In these experiments the electrode was held at +0.80 V for 60 s before each scan.

Table IV shows the effects of the quantity of W bronze redox centers Γ on the BrO_3^- reduction peak. Here, Γ has been determined from the charge under the E_{pc1} peak, which was assumed to correspond to the formation of $H_{0.18}WO_3$. This value is a measure of the number of hydrogen bronze catalytic centers and thus of the thickness of the whole W(VI,V) oxide film. A value

Table III. Voltammetric Parameters for the Reduction of Bromate at Glassy Carbon/W(VI,V) Oxide Electrodes[a]

v/mV s^{-1}	i_{pc}/μA	E_{pc}/V	$i_{pc}v^{-1/2}$/μA $mV^{-1/2}$ $s^{1/2}$
500	311	−0.145	13.9
200	206	−0.120	14.6
100	150	−0.108	15.0
50	108	−0.098	15.3
20	69	−0.092	15.5
10	49	−0.088	15.6
5	35	−0.086	15.6

[a] E_{pc} and i_{pc} are the bromate cathodic peak potential and net current (i.e., after subtraction of the background current), respectively. Experimental conditions are the same as for Figure 7, except that the scan rate, v, is varied.

Table IV. Voltammetric Parameters for the Reduction of Bromate vs Quantity of the W(VI,V) Oxide Film[a]

$10^7\Gamma$/mol cm^{-2}	i_{pc}/μA	E_{pc}/V
0.2	49	−0.115
0.5	72	−0.103
1.4	103	−0.095
2.4	108	−0.098
3.6	105	−0.099
8.2	78	−0.105
24.6	64	−0.110
41.8	51	−0.120

[a] Scan rate = 50 mV s^{-1}; electrode geometric area = 0.071 cm^2; $[BrO_3^-]$ = 2 mM; electrolyte, 2 M H_2SO_4; Γ, the quantity of hydrogen W bronze sites in the W(VI,V) oxide film measured by integration in the absence of bromate.

of (1–4) × 10^{-7} mol cm^{-2} appears to be optimal for catalysis. Markedly thinner or thicker films yield lower bromate reduction currents. The thin films probably do not offer enough catalytic sites to handle the available supply of bromate, while the thicker ones seem to suffer from a resistive barrier to the delivery of electrons (or H atoms) to the catalytic sites. Structural changes are possible as the coverage is increased. The tabulated data show that the film thickness does not affect the peak potential significantly.

Rotating Disk Diagnostic Experiments. Saveant and Andrieux[52-54] have shown that the dynamics of a catalytic modified electrode can be controlled by several factors, alone or in combination. They include (a) analyte transport in solution, (b) analyte diffusion through the W oxide film, (c) electron propagation within the coating, (d) the catalytic reaction at the film–solution interphase or within the film, and the (e) heterogeneous charge transfer rate at the underlying carbon surface.[52-54] The relative importance of these factors generally depends on the film thickness. Rotating disk voltammetry is particularly effective in delineating the limiting elements.

In terms of electrocatalytic efficiency, the ideal system would be one in which the current were limited exclusively by mass transport of the analyte in solution. Such behavior has been observed, for example, for the electrocatalytic oxidation of As(III) on a glassy carbon electrode modified with a thin film of mixed Ru cyanide complexes.[10] For bromate reduction, there is a large barrier to charge transfer at the bare carbon electrode.[29-31] With a sufficient quantity of the oxide, rapid electron motion within the film, and a fast cross-exchange reaction between the substoichiometric W oxides or bronzes and BrO_3^-, the outer surface of the film could act as the electrolysis plane. In this case, diffusion of bromate to the carbon substrate would be negligible, and the current would indeed be limited by convective diffusion of BrO_3^- in the solution. Rotating disk measurements indicate that this limiting case is not followed and that dynamics within the film exert partial control over the rate of catalytic reduction.

(52) Andrieux, C. P.; Dumas-Bouchiat, J. M.; Saveant, J. M. *J. Electroanal. Chem.* **1982**, *131*, 1.
(53) Andrieux, C. P.; Saveant, J. M. *J. Electroanal. Chem.* **1982**, *134*, 163.
(54) Andrieux, C. P.; Saveant, J. M. *J. Electroanal. Chem.* **1982**, *142*, 1.

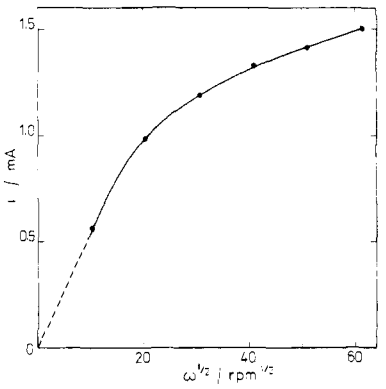

Figure 7. Levich plot for the reduction of 2 mM BrO_3^- in 2 M H_2SO_4 at a rotating glassy carbon/W(VI,V) oxide electrode; geometric area, 0.5 cm^2. Measurements made on the limiting current plateau at −0.35 V.

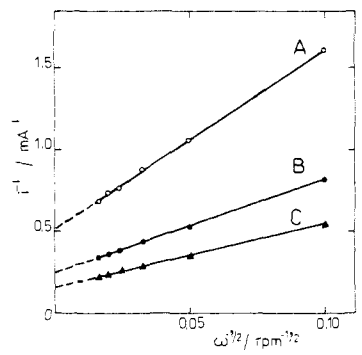

Figure 8. Koutechy–Levich plots for the reduction of bromate at a glassy carbon/W(VI,V) oxide electrode. Bromate concentrations: (A) 2 mM; (B) 4 mM; (C) 6 mM. Other conditions as for Figure 7.

Figure 7 shows the dependence on rotation rate of the limiting current for reduction of BrO_3^- at a modified rotating disk electrode (mRDE) on rotation rate ω. In this case, a glassy carbon disk was coated with the film of optimum thickness (Table IV) to yield a coverage of ca. 240 nm. The limiting current does not vary proportionally with $\omega^{1/2}$, especially at faster rotation. Corresponding Koutecky-Levich reciprocal plots[7,52-54] are shown in Figure 8. Both the slopes and the intercepts of the plots in Figure 8 were inversely proportional to the concentration of BrO_3^-. The fact that there is a positive intercept in each plot clearly indicates a kinetic limitation associated with the film, and the inverse proportionalities of slopes and intercepts with concentration show that the currents were not limited by charge diffusion or the supply of hydrogen to W bronze sites. Therefore, the limiting currents could be described by

$$(i_{lim})^{-1} = (nFAk\Gamma C^b)^{-1} + (i_L)^{-1} \quad (1)$$

where i_L is given by the Levich equation,[33] k is the charge-transfer rate constant for the cross-exchange reaction, Γ is the surface concentration of the hydrogen W oxide bronze sites present in the film, and C^b represents the bulk concentration of BrO_3^-. The other symbols have the usual significance.

Of the five dynamic factors given above, we now know that (e) does not occur at all, that (a) influences the catalytic rate strongly at low rotation rates, but not at high rates, and that (c) appears not to be limiting at the optimal thickness of coating. Thus, factors (b) and (d) seem to be the source of the kinetic limitation imposed by the film. In the terminology of Saveant et al.,[52] we therefore have case R, if the cross-exchange is the sole limiting factor; or we have cases R+S or SR, if cross-exchange and substrate diffusion are rate-controlling in concert. The concentration profiles corresponding to these various cases are shown in Figure 9.

The diagnostic criteria described by Saveant and co-workers[52-54] for the various limiting behaviors in the catalysis of electrochemical reactions at redox polymer electrodes cannot be applied fully in the present case. First, due to total irreversibility of the BrO_3^- reduction at bare carbon substrate, the possible appearance of a

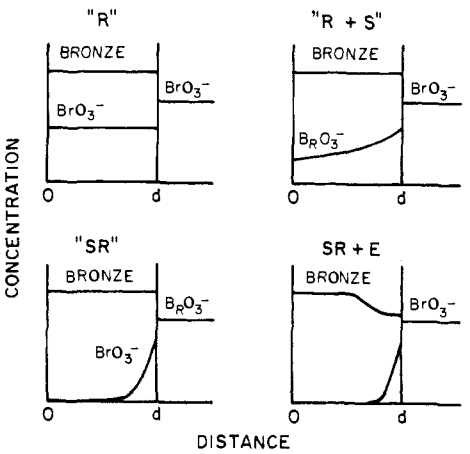

Figure 9. Concentration profiles illustrating the dynamic regimes during the reduction of bromate via hydrogen bronze/W(V) centers in a film at a rotating disk. The electrode–film boundary is at zero distance; d is the film thickness. The profile of bromate in the solution (beyond d) corresponds to a very high rotation rate.

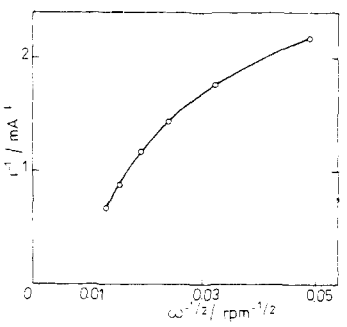

Figure 10. Nonlinear Koutecky–Levich plot for the reduction of bromate at thin W(VI,V) oxide film ($\Gamma = 1.7 \times 10^{-8}$ mol cm^{-2}). Other conditions as for Figure 8.

second reduction wave (a diagnostic criterion for the R subcase[52]) corresponding to the direct reduction of BrO_3^- at the electrode surface could not be considered here. Thus, the "pure" subcase R cannot be definitively ruled out, since bromate is likely to diffuse easily into the porous, hydrated W(VI,V) oxide coating, i.e., to have a diffusion coefficient comparable to its diffusion coefficient in the bulk 2 M H_2SO_4 solution. The other candidate subcases, SR and R + S (Figure 9), differ in the degree to which the cross-exchange zone extends into the film. In case SR, the analyte flux is totally consumed in a narrow region of the coating adjacent to the solution, whereas in subcase R + S, the bromate concentration profile extends from the film–solution interphase to the electrode surface.[52]

Voltammetric data in Table IV show clearly that very thin coatings are not catalytically efficient. Apparently there are not enough redox centers, and the bromate concentration at the carbon surface is not drawn down to a negligible value. With thin films, the R or R + S cases are therefore the most probable. For bromate reduction at the optimum thickness (Table IV), the number of catalytic sites is increased, and the system may move into subcase SR. The catalytic reaction seems to be fast enough (Figure 6 and Table III) for mutual compensation[52-54] between the diffusion and the reaction of BrO_3^- in the film to be achieved.

The value of $k\Gamma$ was estimated from the intercepts of the plots in Figure 8.[7,52] The result was ca. 2×10^{-4} cm s^{-1}, which is a rather moderate intrinsic rate of heterogeneous charge transfer. The rate constant was independent of the bulk BrO_3^- concentration, at least in the range from 2 to 6 mM. The experiments were done for a modified electrode that upon integration of the E_{pc1} peak yielded a surface charge of 3.8 mC cm^{-2}, corresponding to 2.2×10^{-7} mol cm^{-2}.

The Koutecky–Levich plots for very thin W(VI,V) oxide films ($\Gamma = 1.7 \times 10^{-8}$ mol cm^{-2}) were clearly nonlinear (Figure 10). This result is not expected and is not understood. Thinner films

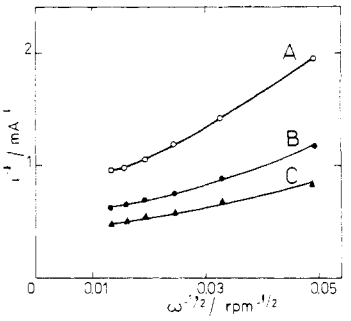

Figure 11. Koutecky–Levich plots for the reduction of bromate at thick W(VI,V) oxide film (Γ = ca. 35×10^{-7} mol cm^{-2}) with the following bromate concentrations: (A) 2 mM; (B) 4 mM; (C) 6 mM. Other conditions as for Figure 8.

are even more hydrated and permeable than the optimal ones, so the bromate diffusion factor cannot be rate-limiting. It is apparent from chronocoulometric experiments that the "diffusion" of charge is moderately fast, hence no charge propagation-limited condition should apply either. Perhaps imperfections in the film structure perturb the convective–diffusion pattern near the electrode. Alternatively, there may be some change in the kinetics of the cross-exchange reaction.

In the case of the thick W(VI,V) oxide films, the limiting rates of charge propagation and bromate diffusion in the coating are lower, and the limiting catalytic reaction rate could become, relative to them, not a strongly rate-determining factor.[52,54] Thus, the observed current may be under kinetic control of both diffusion processes in the film (subcases SR + E or S + E in the Saveant–Andrieux notation). Neither the slopes nor the intercepts of the lines in the Koutecky–Levich reciprocal plots remain inversely proportional to the bulk concentration of BrO_3^-, even though they are still BrO_3^- concentration dependent (Figure 11). The lines A, B, and C in Figure 11 are actually nonlinear, so limiting slopes and intercepts at low ω were considered in the argument above. On the basis of the diagnostic criteria developed by Saveant et al.,[52-54] we can conclude from the nonlinearity that the pure S + E limiting behavior does not apply. The subcase SR + E (Figure 9) seems most likely.

In summary, we think it most probable that these systems progress from subcase R in very thin films, through subcase S + R at suboptimal thicknesses, to case SR at optimal thickness, and then to case SR + E at superoptimal thickness. This pattern is an expected result of increasing loading of the oxide. It may be abetted by declines in the overall effective diffusion coefficients for bromate and for electrons (or H atoms) with increasing thickness. We have already indicated that the film becomes denser as it grows thicker.[24]

Mechanism of Catalysis. Because our W(VI,V) oxide films give a strong catalytic effect, a more specific chemical reactivity than simple outer-sphere electron transfer is probably involved.[55,56] It has been pointed out that the best electrocatalysts react through inner-sphere pathways,[55] e.g., with the participation of ligand-bridged transition states. Since the outermost portions of the film are not only hydrated but are also positively charged (because WO_3 tends to form WO_2^{2+} on the surface[35]), the initial step might include formation of a complex in which bromate pairs with WO_2^{2+} and displaces a water molecule in its inner coordination sphere. Both the existence of the cationic WO_2^{2+} and the efficiency of the proposed association would require extensive hydration[35] and high porosity[34] in the oxide. As already mentioned, redox transitions in such porous and hydrated coatings lead to the formation of hydrogen W bronzes, which are known to be the most reactive forms of nonstoichiometric W oxides toward catalytic reductions.[44]

It is not appropriate, however, to attribute the catalytic activity of the W(VI,V) oxides solely to the hydrogen tungsten bronzes

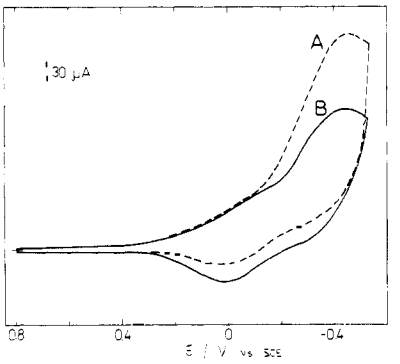

Figure 12. Cycic voltammograms for W(VI,V) oxide film on glassy carbon that, after preparation, was heated in an oven for 4 h at 80 °C. Curves A and B recorded in 2 M H_2SO_4, but (A) upon addition of 2 mM bromate. Geometric area, 7.1 mm^2; scan rate, 50 mV s^{-1}.

in the hydrated portions of the film. The less hydrated substoichiometric lower W oxides (WO_{3-y}) that are formed at more negative potentials are also of concern. An additional experiment bears on the point. It is well-known that the extent of hydration of WO_3 depends on temperature.[36] For example, the anodic oxide films on W formed in strong acids at 70 °C are predominantly monohydrates, $WO_3 \cdot H_2O$.[35] In order to dehydrate the oxide film to monohydrate form,[24] the modified electrode was heated for 4 h at 80 °C. As is evident from Figure 12 (curve B), the voltammetric peaks for the hydrogen tungsten bronzes almost completely disappeared in favor of a broad peak at about −0.42 V. Although the redox transitions in the baked coating were slow, as evidenced by the separation of the respective oxidation and reduction peaks (Figure 12B) the film continued to exhibit catalytic activity toward bromate (Figure 12A). The bromate peak was, however, relatively smaller and was shifted ca. 350 mV toward more negative values, when compared to the behavior at the film with hydrogen tungsten oxide bronze sites (Figure 6). Therefore, catalysis by the dehydrated W(VI,V) oxide film was not pursued.

By analogy with the homogeneous kinetics of the reduction of bromate by vanadium(IV) in acid medium,[57] our catalytic reduction of BrO_3^- is presumed to involve the formation of a bromate–hydrogen W bronze complex, the decomposition of which is rate-determining

$$xBrO_3^- + (H_xWO_2^{2+}, H_xWO_3) \overset{\text{fast}}{\rightleftharpoons} [H_xWO_2^{2+} \cdot xBrO_3^- \cdot H_xWO_3] \quad (2)$$

$$[H_xWO_2^{2+} \cdot xBrO_3^- \cdot H_xWO_3] \overset{\text{slow}}{\longrightarrow} xH_2O + xBrO_2\cdot + (WO_2^{2+}, WO_3) + xe^- \quad (3)$$

The assumption is made that bromate can react with either surface cationic ($H_xWO_2^{2+}$) or neutral (H_xWO_3) forms of the hydrogen W oxide bronze. The reducing power of adsorbed hydrogen[44] is emphasized here. In addition, these oxides, even when oxidized,[58] are also slightly substoichiometric, i.e., of the WO_{3-y} type, and contain oxygen vacancies.[25,28] The parallel reaction can be written as follows:

$$yBrO_3^- + WO_{3-y} \rightleftarrows [yBrO_3^- \cdot WO_{3-y}] \rightarrow yBrO_2\cdot + WO_3 + ye^- \quad (4)$$

and would be rate limiting at more negative potentials where WO_{3-y} predominates.

Thus, as in the case of vanadium,[57] the charge-transfer intermediate may also involve bonding between the 2p orbital of oxygen

(55) Anson, F. C. *J. Phys. Chem.* **1980**, *84*, 3336.
(56) Andrieux, C. P.; Dumas-Bouchiat, J. M.; Saveant, J. M. *J. Electroanal. Chem.* **1978**, *87*, 39.
(57) Fuller, C. W.; Ottaway, J. M. *Analyst* **1969**, *94*, 32.
(58) Witzke, H.; Cartmell, D. K.; Deb, S. K. Electrochemical Society Fall Meeting, Las Vegas, NV, 1976; Extended Abstract No. 202.

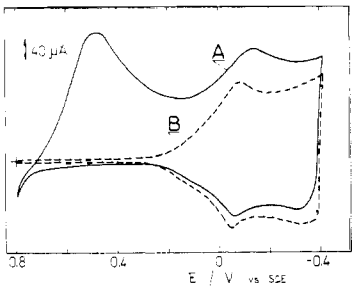

Figure 13. Cyclic voltammograms at the W(VI,V) oxide modified electrode recorded in the presence (A) and absence (B) of 1 mM Br_2. Electrolyte, 2 M H_2SO_4; geometric area, 7.1 mm^2; scan rate, 50 mV s^{-1}; Br_2 concentration, 1 mM (curve A).

on the bromate and vacant 5d orbitals of W, so that the oxygen transfer is simply a matter of breaking the Br–O bond.

Nevertheless, the slow step involves oxygen transer from bromate to the nonstoichiometric W oxide centers to produce WO_3 (or WO_2^{2+}) and $BrO_2^{\bullet}$.

By analogy with the known homogeneous chemistry,[57,59] the remaining Br–oxo intermediates, such as $BrO_2^{\bullet}$, $HBrO_2$, and HOBr, are believed to undergo rapid electroreduction to yield free Br_2. The latter species is not a final product, because at the potentials of the catalytic reduction, Br_2 must be reduced to Br^-. This expectation was verified by an additional experiment in which 1 mM Br_2 in 2 M H_2SO_4 was reduced at the modified electrode. The peak resulting from the reduction at the underlying carbon substrate occurred at 0.55 V (Figure 13A). The reduction of the remaining (unreacted) bromine flux was clearly completed by the reduced W(VI,V) oxide film (compare curves A and B at ca. –0.1 V in Figure 13). Thus, it is plausible to assume that under these conditions bromate acts as a six-electron oxidant. The statement cannot be, however, independently verified from the heights of voltammetric peaks. Due to the uncertainty of the mechanisms for the BrO_3^- reduction on Pt or Hg in acidic media,[29,30,60] it was impossible either to find accurate diffusion coefficients or to decide whether the process involves five or six electrons.

Under certain conditions, particularly in strong acids, Br_2 could be a product of a homogeneous chemical reaction[60]

$$BrO_3^- + 5Br^- + 6H^+ \rightarrow 3Br_2 + 3H_2O \qquad (5)$$

Indeed, when our catalytic experiment was performed in 4 M H_2SO_4 containing 10 mM BrO_3^-, we found that after the first cathodic scan (Figure 14, curve 1), the Br_2 reduction peak was clearly visible in the reverse scan (at about 0.5 V in Figure 14, curve 1). Upon repetitive cycling (50 mV s^{-1}, scan rate, each experiment interrupted for 30 s at 1.0 V), the Br_2 reduction peak was visible in both negative and positive scans (Figure 14, curves 1 and 2) and exhibited a tendency to grow steadily. Obviously the observed behavior was due to the Br_2 generated (via eq 5) in the vicinity of the electrode surface.

The effects of Br_2 generation in the more concentrated H_2SO_4/BrO_3^- solutions cannot be observed in mRDE experiments at 900 rpm or higher, since the liberated Br_2 is convectively

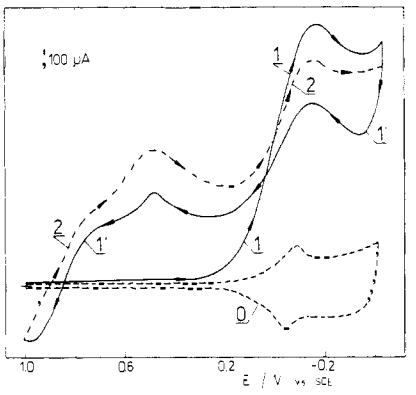

Figure 14. Cyclic voltammograms for the reduction of bromate at a glassy carbon electrode modified with the W(VI,V) oxide coating. Curve 0 represents the cyclic voltammogram of the modified electrode in 4 M H_2SO_4 only. For other curves bromate is present at 10 mM. After the first scan (1) the reverse one (1′) and the second voltammetric scan (2) were recorded. Scan rate, 50 mV s^{-1}; geometric area, 7.1 mm^2.

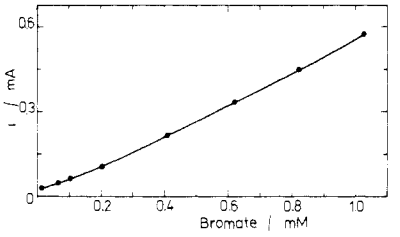

Figure 15. Voltammetric working curve at the W(VI,V) oxide coated glassy carbon electrode. Other conditions are the same as for Figure 7.

transported away from the electrode and its bulk concentration is negligible. From the viewpoint of electroanalytical methodology, this feature allows one to avoid complications with the onset of Br_2 formation. In practice 2 M H_2SO_4 electrolytes containing bromate at levels not exceeding 6 mM are recommended. Figure 15 shows a working curve wherein the analytical current was taken as the difference between the peak current at about –0.095 V and the background current measured at the W(VI,V) oxide modified electrode in blank electrolyte at the same potential. The plot shows a positive deviation from linearity at lower concentrations; this may be due to relatively larger partitioning of BrO_3^- into the film at lower concentrations. The reproducibility of 7% (relative standard deviation) in nine replicate cyclic voltammetry experiments was obtained with an electrode of optimal thickness, i.e., 2000–2500 Å. All of the experiments were performed on 0.4 mM BrO_3^- in 2 M H_2SO_4 over a 2-day period with a 50 mV s^{-1} scan rate. For uninterrupted work over periods longer than hours, the electrodes showed poorer reproducibility. In the above experiments, the electrode was held at 0.8 V for 90 s prior to each scan.

Even when the bromate catalysis or electrochromism are not particularly of interest, this modified electrode may have value. The surface seems to possess a fairly general catalytic activity for highly irreversible cathodic reactions in which the oxygen content of the reaction product is lower than that of the reactant. Examples include hydrogenation of *p*-nitrophenol and reductions of chlorate or arsenate. More detailed studies and applications are under investigation at present.

Acknowledgment. This work was supported by the U.S. Department of Energy, Division of Materials Sciences, under Contract DE-ACO2-76ER01198, administered by the Materials Research Laboratory of the University of Illinois. Surface measurements were carried out in the Center for Microanalysis of Materials of the Materials Research Laboratory. This facility is also supported by the Department of Energy under the same contract. The authors thank Nancy Finnegan and Judith Baker for technical assistance.

(59) Thompson, R. C.; Noyes, R. M.; Field, R. J. *J. Am. Chem. Soc.* **1971**, *93*, 7315.
(60) Desideri, P. G.; Lepri, L. *J. Electroanal. Chem.* **1969**, *22*, 265.